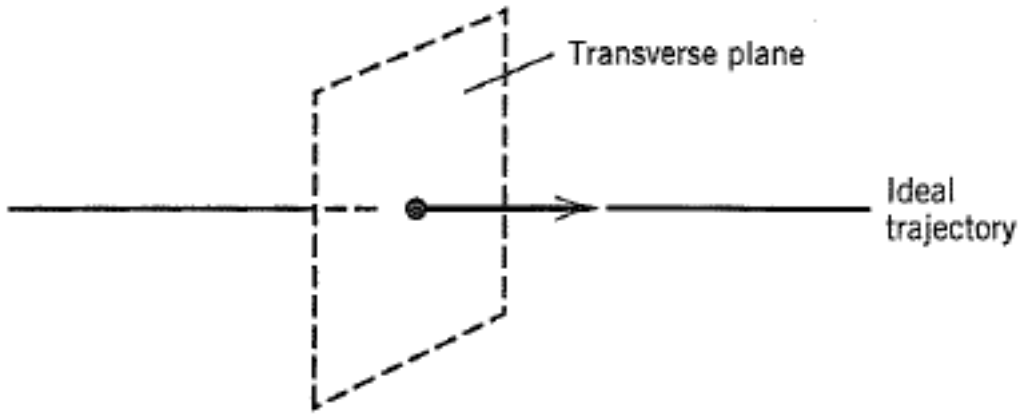

Figure 3.1. Characterization of transverse and longitudinal degrees-of-freedom of particle motion.

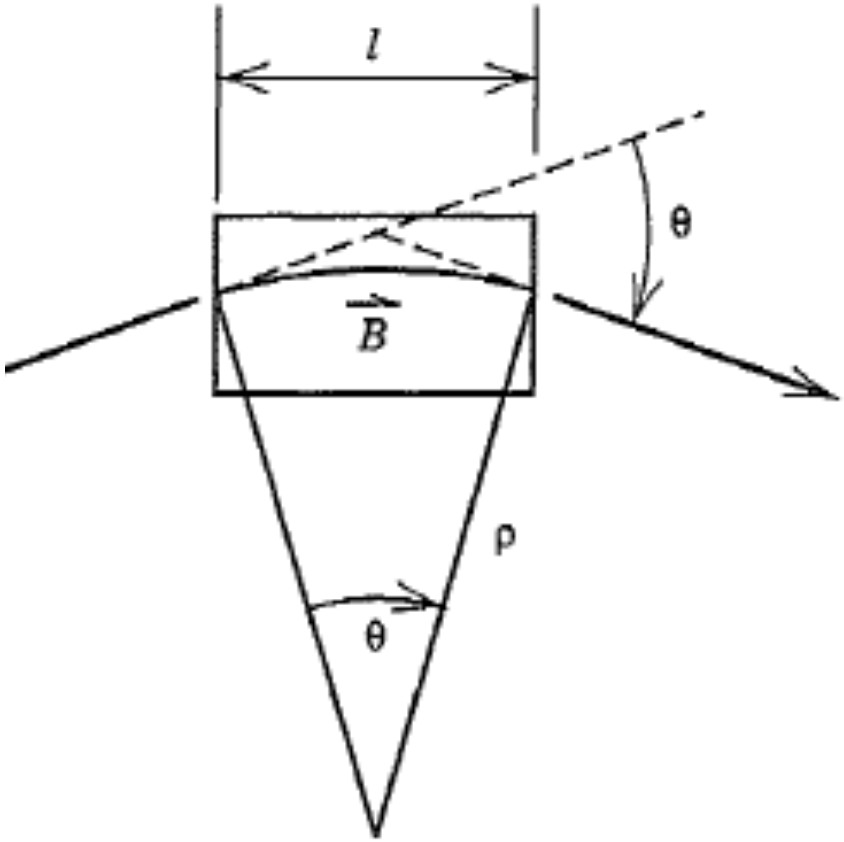

Figure 3.4. Deflection of particle by tl magnetic element.

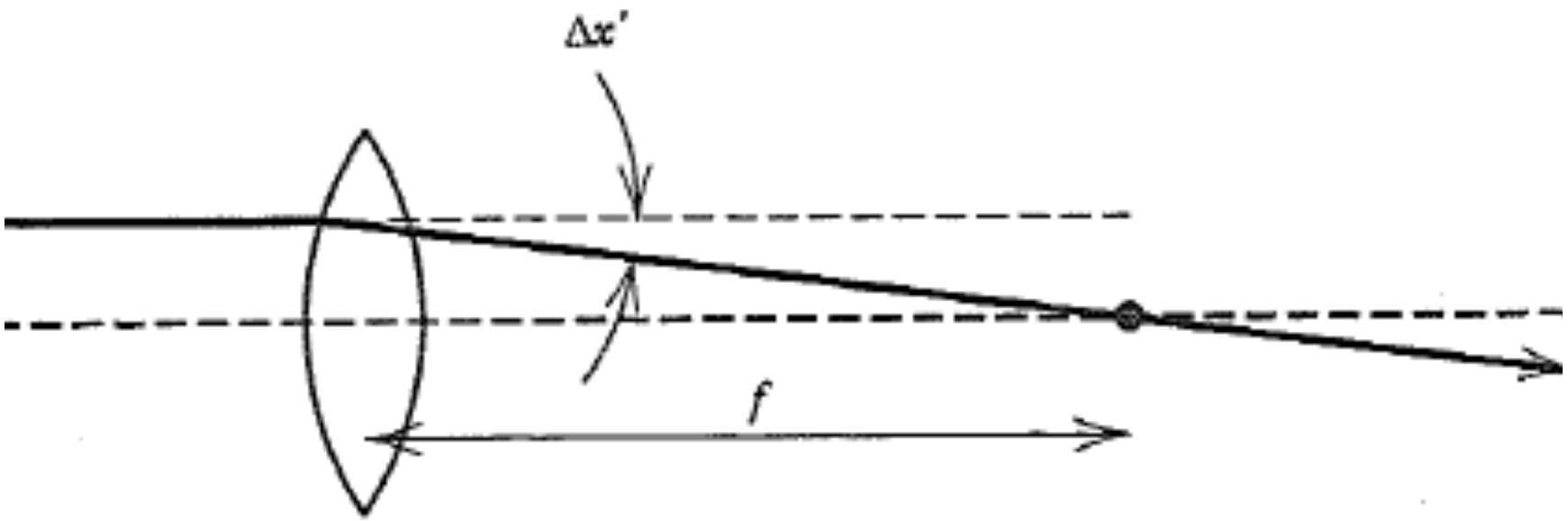

Ray initially parallel to the optical axis is bent by a convex lens causing it
ocal point a distance f away.

$$\begin{pmatrix} x \\ x' \end{pmatrix}_{\text{out}} = \begin{pmatrix} 1 & 0 \\ -\frac{1}{f} & 1 \end{pmatrix} \begin{pmatrix} x \\ x' \end{pmatrix}_{\text{in}}. \qquad (3$$

r a concave lens, the focal length is of opposite sign. In this language, ›gress of a ray through the interlens space of length L is given by

$$\begin{pmatrix} x \\ x' \end{pmatrix}_{\text{out}} = \begin{pmatrix} 1 & L \\ 0 & 1 \end{pmatrix} \begin{pmatrix} x \\ x' \end{pmatrix}_{\text{in}}. \qquad (3.$$

erefore, the matrix corresponding to transport of the ray through fir ıcave lens, then a drift, and then a convex lens may be written as

$$\begin{pmatrix} 1 & 0 \\ -\frac{1}{f} & 1 \end{pmatrix} \begin{pmatrix} 1 & L \\ 0 & 1 \end{pmatrix} \begin{pmatrix} 1 & 0 \\ \frac{1}{f} & 1 \end{pmatrix} = \begin{pmatrix} 1+\frac{L}{f} & L \\ -\frac{L}{f^2} & 1-\frac{L}{f} \end{pmatrix}. \qquad (3.$$

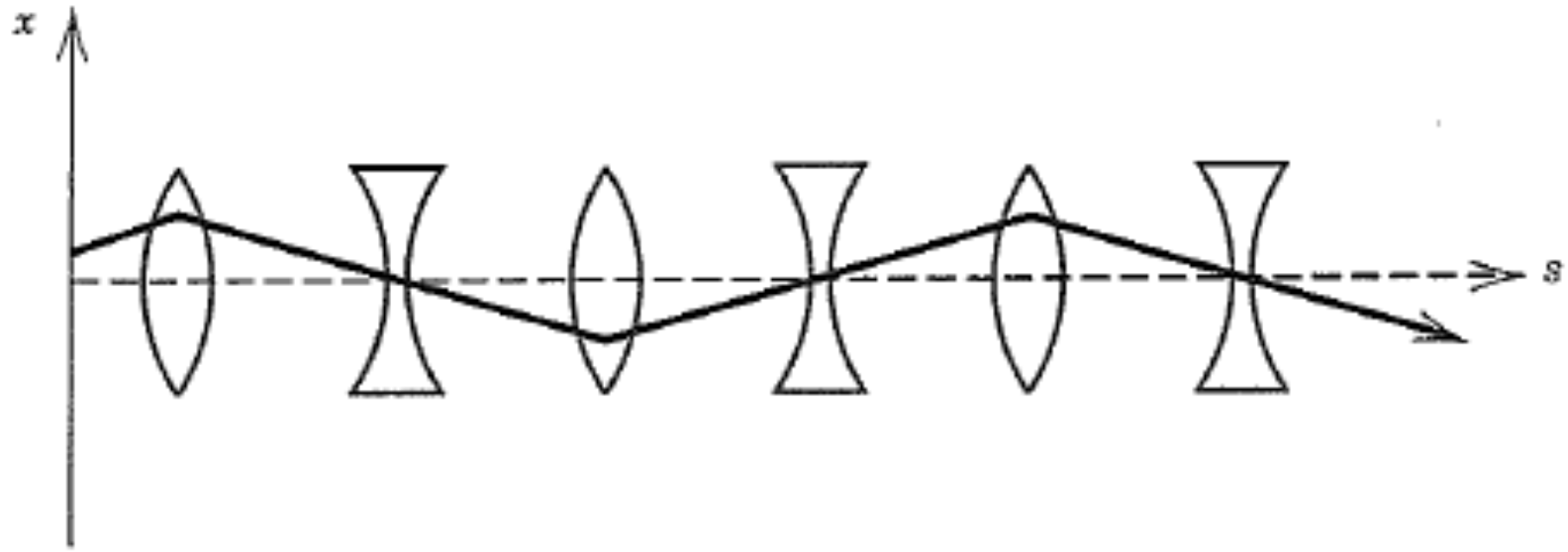

ıre 3.6. Example of a particle oscillation through a system of lenses where $f = L / 2$. Th
mum displacement is independent of the size of the accelerator.

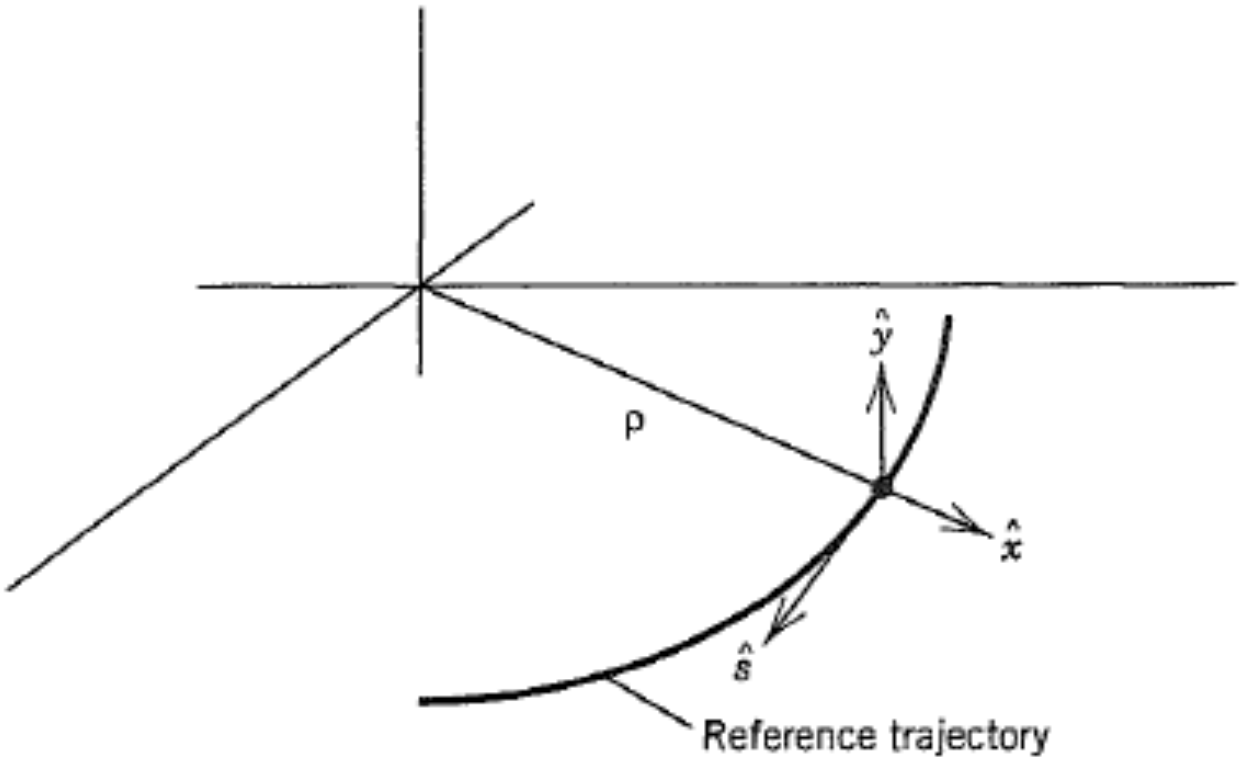

Figure 3.7. Coordinate system for development of equation of motion.

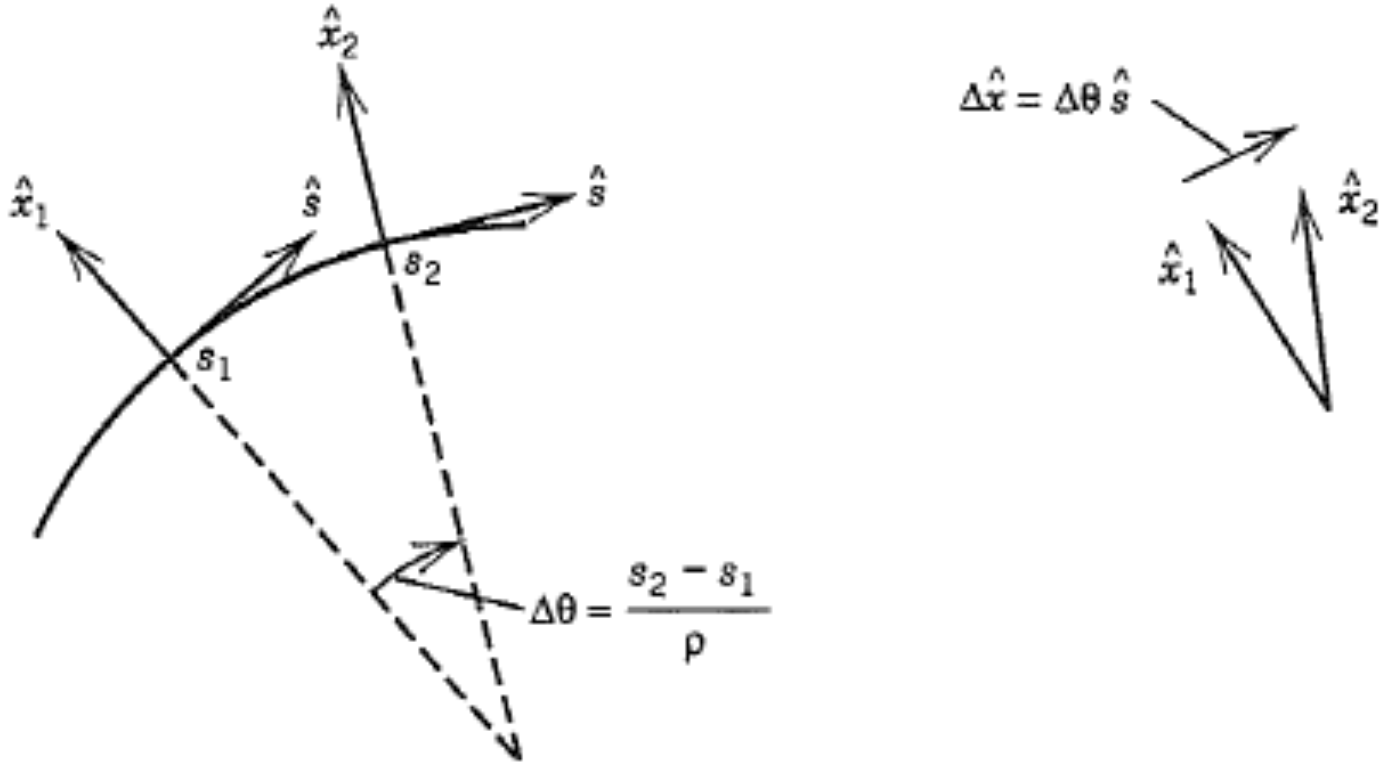

Figure 3.8. Time rate of change of unit vector $\hat{x}$.

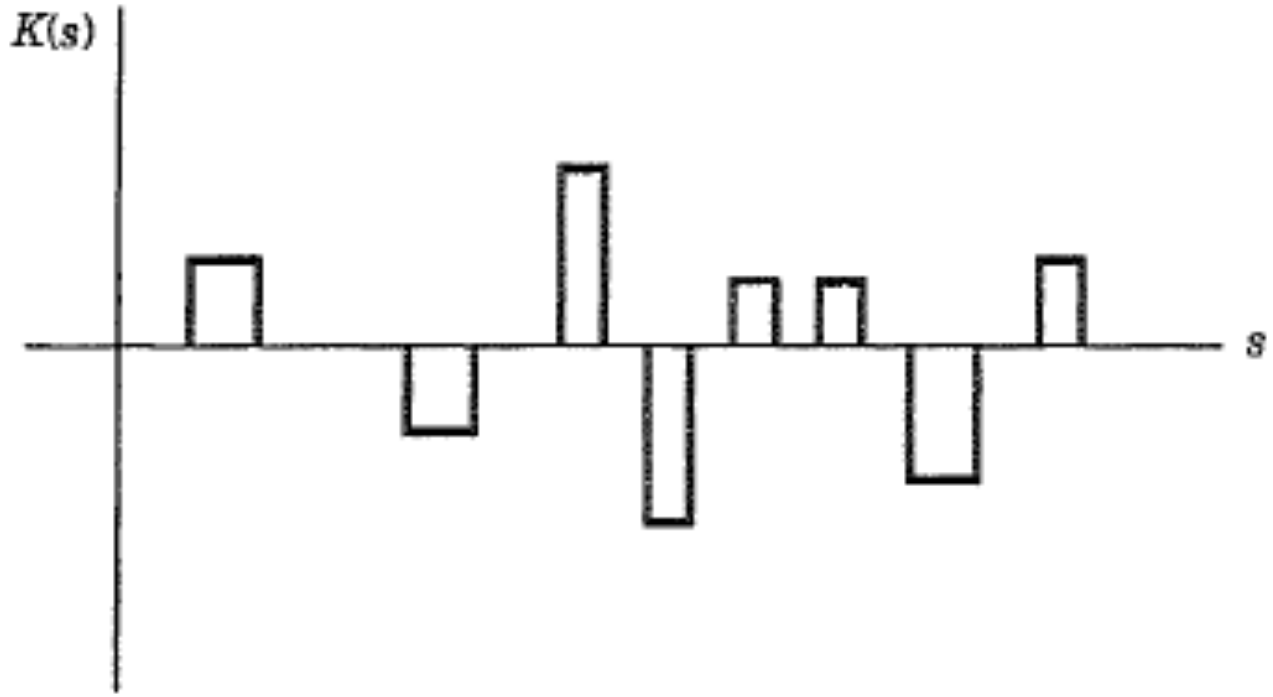

.10. The spring constant K varies with position, but is normally constant wit components of the accelerator.

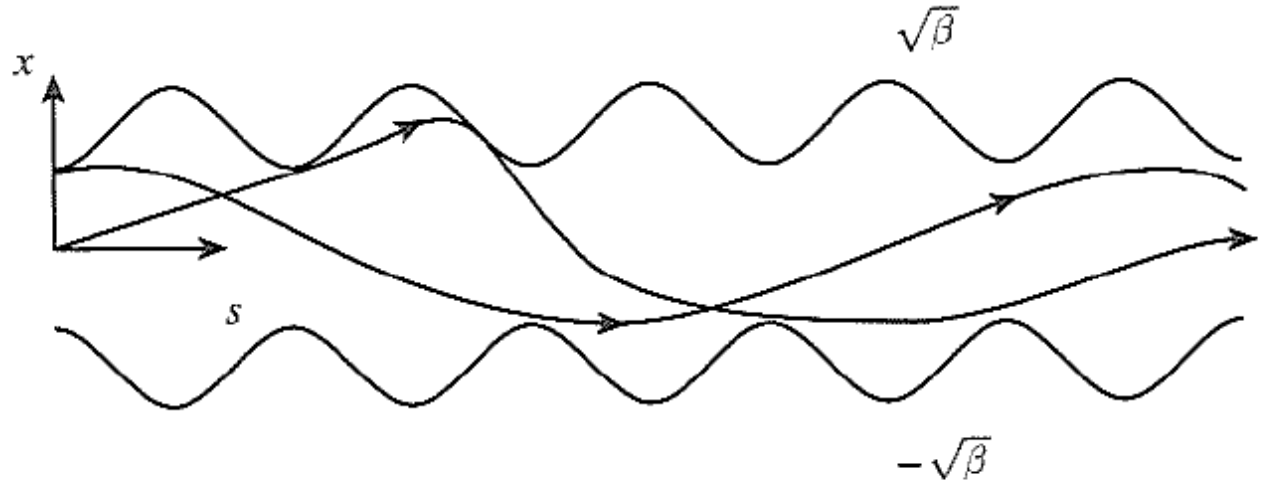

FIGURE 2.9 Betatron oscillations. In a ring accelerator, each transverse coordinate x of a particle oscillates as a function of path length s within an envelope described by the so-called β-function. In the example illustrated, focusing quadrupoles are located at the peaks and defocusing magnets are located at the troughs of the β- function. A cosine-like trajectory starting at $s = 0$ and a sine-like trajectory starting at $s = 0$ are shown [After M Sands, "The Physics of Electron Storage Rings: An Introduction", SLAC-r-121, 35 (1970)]

Table 2: Summary of the main LHC beam and machine parameters for 2015. It should be noted that the emittance values in collision are optimistic and assume emittance growth only from IBS with values from Ref. [15]. If the scrubbing is not fully successful, larger emittances should be expected. Furthermore, the intensity in collision assumes a 95% transmission of the injected intensity. It should also be noted that the 2012 mm kept collimator settings in collision might still be modified to achieve a larger margin for machine protection between the TCDQ and the TCTs.

Parameter	Unit	Value at injection	Value at collision
Beam energy	TeV	0.45	6.5
β^* at IR1/IR2/IR5/IR8	m	11 / 10 / 11 / 10	0.8 / 10 / 0.8 / 3
half crossing angle at IR1/IR2/IR5/IR8	μrad	-170 / 170 / 170 / 170	-145 / 120 / 145 / -250
Tunes (H/V)	–	64.28/59.31	64.31/59.32
Parallel separation at IR1/IR2/IR5/IR8	mm	2 / 2 / 2 / 3.5	0.55 / 0.55 / 0.55 / 0.55
Normalized emittance (BCMS/nominal)	μm	$\geq$ 1.3 / $\geq$ 2.4	$\geq$ 1.7 / $\geq$ 2.7
Total number of bunches (BCMS/Nominal)	–	$\leq$ 2604 / 2748	
Number of bunches colliding at IR1/5 (BCMS/Nominal)	–	$\leq$ 2592 / 2736	
Bunch intensity	p	$\leq 1.3 \times 10^{11}$	$\leq 1.2 \times 10^{11}$
Bunch length (4σ)	ns	1.0–1.2	1.0–1.25
Collimator settings	–	2012 mm kept	2012 mm kept

accelerator located at equivalent values of the amplitude function, we would expect the rms value of the closed orbit distortion to be larger than the preceding figure by a factor of order $N^{1/2}$ with the placement error δ also reinterpreted as an rms value. In the Tevatron, $N \approx 100$, so we come to an estimate of 10 mm for the rms orbit distortion due to quadrupole placement errors, and we would expect peaks larger than the rms by some factor on the order of 3 or 4, depending upon the distribution. As a consequence, we need some means of correcting steering errors as a basic design feature in synchrotrons of this scale.

Correction of closed orbit distortions can be carried out with the aid of a set of independently powered steering dipole magnets. The same set of steering dipoles can be used to make intentional closed orbit distortions to facilitate a variety of accelerator functions. More rigorous and quantitative calculations of the above are the subject of some of the problems at the end of the chapter.

As a final note, referring to Equation 3.146, we observe that there is no closed orbit if the tune is an integer. This is the most elementary example of a resonance. Of course, we didn't need to go through any algebra to find that out. If the tune were an integer, the steering errors would just reinforce from turn to turn until the oscillation amplitude became large enough to strike the walls of the vacuum chamber. The implication in the formula that the orbit goes to infinity is just an artifact of our approximations. But since infinity is only a few centimeters away, the approximations are pretty good.

3.4.2 Focusing Errors and Corrections

A gradient error would be expected to alter the tune of a circular accelerator. Let there be a single gradient error equivalent to a thin lens quadrupole with focal length f. The matrix M for a single turn is then

$$M = M_0 \begin{pmatrix} 1 & 0 \\ -\frac{1}{f} & 1 \end{pmatrix}, \tag{3.147}$$

where M_0 is the matrix for the ideal ring. From the trace of M it follows that

$$\cos 2\pi\nu = \cos 2\pi\nu_0 - \frac{1}{2}\frac{\beta_0}{f}\sin 2\pi\nu_0, \tag{3.148}$$

where ν and ν_0 are the new and old tunes respectively, and β_0 is the original amplitude function at the point of the perturbation. For the ideal ring, presumably ν_0 is real by design. But depending on the sign and magnitude of the gradient error term, ν can become complex; that is, the motion can become unstable. Since, for small magnitudes of the gradient error term, the

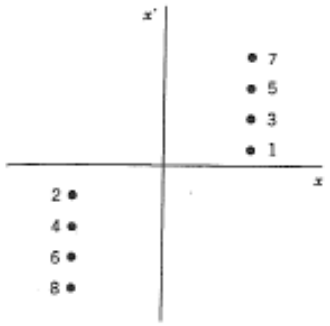

Figure 3.18. Phase space development of particle trajectory in presence of half-integer resonance.

instability will occur for ν near an integer or half integer, these instabilities are called half-integer resonances. There will be a range of values of ν_0 for which the motion is unstable; this range is called a *stopband*.

Just as in the case of dipole error resonances, we didn't need to use any algebra to demonstrate that quadrupole errors can produce resonance effects. Figure 3.18 represents the phase space history of a particle on successive turns as it passes the gradient error. The initial motion, in the absence of the error, was one in which the tune was an odd multiple of one-half. Successive passages of the gradient error just add constant vectors parallel to the vertical axis.

If the tune is not near a half-integer and the perturbation is sufficiently small, we can obtain a useful expression for the tune shift due to a gradient error by writing

$$\nu = \nu_0 + \delta\nu \tag{3.149}$$

and expanding the cosine term on the left hand side of the last equation. The result is

$$\delta\nu = \frac{1}{4\pi}\frac{\beta_0}{f}. \tag{3.150}$$

If there is a distribution of gradient errors, this last result generalizes to

$$\delta\nu = \frac{1}{4\pi}\sum_i \frac{\beta_i}{f_i} \to \frac{1}{4\pi}\oint \frac{\beta(s)B'(s)}{(B\rho)}\,ds \tag{3.151}$$

and is the lowest order (in gradient error) approximation to the tune shift.

In analogy with steering errors and corrections, one can make adjustments to the tunes of the accelerator by intentionally introducing perturbations on the gradients. The capability to adjust the tune is essential to modern high